Wide Angle Mirror System Design for Distortionless Imaging of the Sky

Hannah VanWingen[1], Michael Kosch[2], Mark Moldwin[3]

[1]University of Michigan-Ann Arbor, Department of Physics, Michigan, United States; hvanova@umich.edu
[2] South African National Space Agency (SANSA) Space Science, Hermanus, South Africa; mkosch@sansa.org.za
[3] University of Michigan-Ann Arbor, Department of Climate and Space Sciences and Engineering, Michigan, United States; mmoldwin@umich.edu

Abstract

Imaging using all-sky lenses of 180° field of view has a long tradition in atmospheric airglow and auroral science. For a vertically mounted camera, the traditional fish-eye lens systems are linear in local zenith and azimuth angle. Hence, they introduce significant radial distortion, especially toward the horizon of the image. A novel convex mirror shape that removes the fish-eye distortion from the image and keeps fixed resolution over the entire sky at a chosen altitude (e.g., 100 km) was developed in the early 90s. However, the local sky zenith in the image is blocked by the camera itself as it is situated looking down onto the mirror. We have solved this problem by using two convex mirrors with special profiles. However, this convex mirror system suffers from significant focusing issues. We use Snell's law of reflection, simple mathematics and straight-line ray tracing to design a corrected wide angle mirror system (WAMS) using two concave mirrors. The design provides a real time achromatic transform while implementing a uniform spatial sky resolution and optimizing focus throughout the field of view.

Design & Methods

When all-sky images are processed using a standardized grid, the spatial resolution is reduced, especially toward the horizon. Fig. 1 illustrates the geometry from which the transform Eq. 1 is derived to eliminate radial distortion and control spatial resolution within the image. By applying this transform to the WAMS, the final image will appear to the viewer as if they are located at the center of the Earth.

$$\tan(\theta) = \frac{(h+r)\sin(\varepsilon)}{(h+r)\cos(\varepsilon) - r}$$

Eq.1. Relationship between θ and ε when h and r are constant.

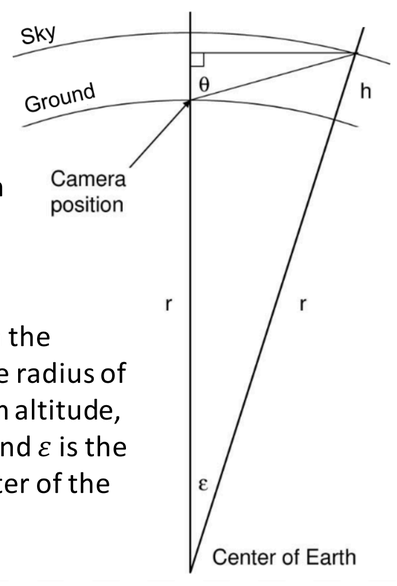

Fig.1. Geometry from which the transform is derived. r is the radius of the Earth, h is the transform altitude, θ is the local zenith angle, and ε is the angle subtended at the center of the Earth.

Our design involves concave mirrors as they compress the focal range over which an object appears in the image. Furthermore, by using two mirrors we create a compact system where camera rays span from the local zenith to the horizon without obstructions.

References

[1] Kosch M., Pedersen T., Esposito R. 2009. Wide angle mirror system design for distortionless imaging of the sky. Optical Society of America, Applied Optics. 48 (24): 4703-4708.
[2] Hough G., Scourfield M. W. J. 1991. WAND auroral imager for SANAE. S. Afr. J. Antarct. Res. 21 (113).

Design & Methods (Cont.)

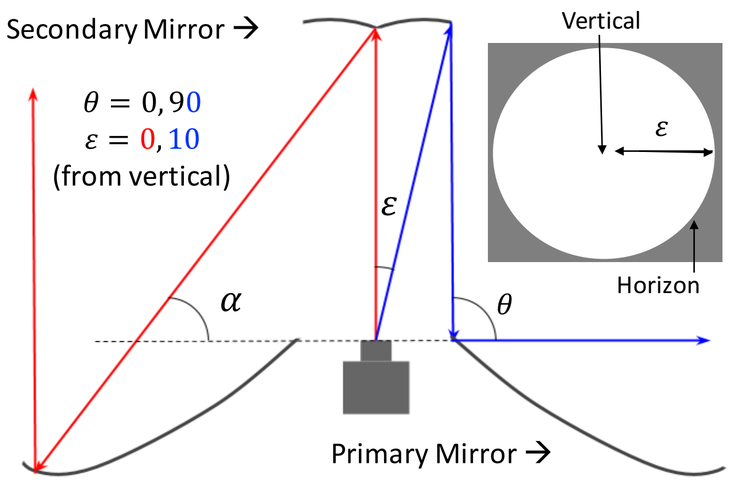

Fig.2. Necessary boundary conditions for an arbitrary primary mirror to adhere to the spatial transformation in Eq. 1. The system is rotationally symmetric about the camera. Values for α (measured from horizontal) are dependent on the properties of a predefined secondary mirror and are limited so that rays reflecting from the secondary mirror do not interfere with the camera.

For any controlled secondary surface, we approximate a primary surface based on the necessary θ to ε transform conditions (Fig. 2). For the widest view we consider $\varepsilon \approx \pm 10°$, but $\varepsilon \approx \pm 3°$ is sufficient for real applications.

Secondary A [cm]: *radius = 23.5; center = (6.9, 27.5)*
Secondary B [cm]: *radius = 20.8; center = (6, 28)*

These are possible solutions to the non-unique but constrained problem. The entire design must fit within a 1 meter wide hemispheric dome, and all camera and mounting equipment must fit within the hollow center of the primary mirror.

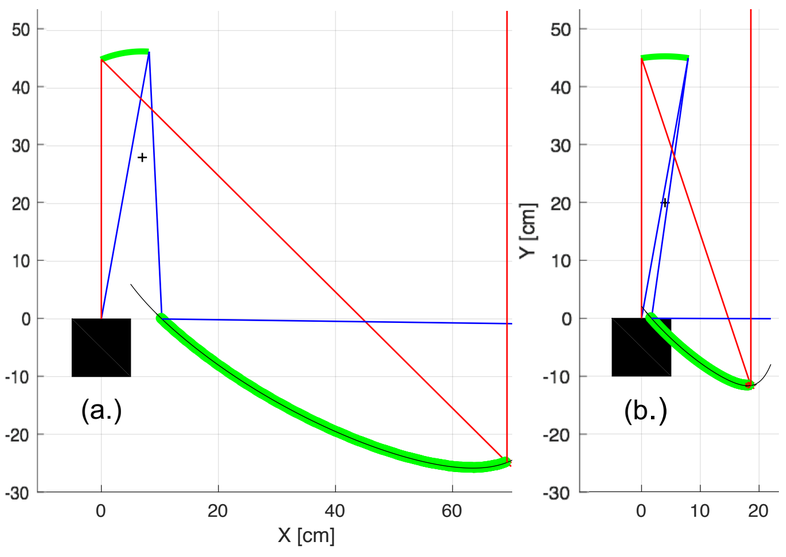

Fig.3. An illustration of iterations for alternative secondary mirror dimensions. Although 3a. and 3b. preserve the transform relationship, they are non-ideal designs. Design 3a. does not fit the dome dimensions and the primary mirror for design 3b. interferes with the camera.

$$primary\ mirror\ slope = -\frac{1}{\tan\left(45 - \frac{1}{2}(\alpha - \theta)\right)}$$

Eq.2. Slope equation relating the reflection of rays from the secondary mirror and the all-sky transform Eq. 1.

Acknowledgements

Thank you to the South African National Space Agency for making the resources available for this project.

To continuously connect each primary mirror slope segment and create a smooth estimated surface, we implement a piecewise quadratic approximation shown in green for Fig. 3 and Fig. 4. With this method we calculate intersection points and assign slope values using Eq. 2.

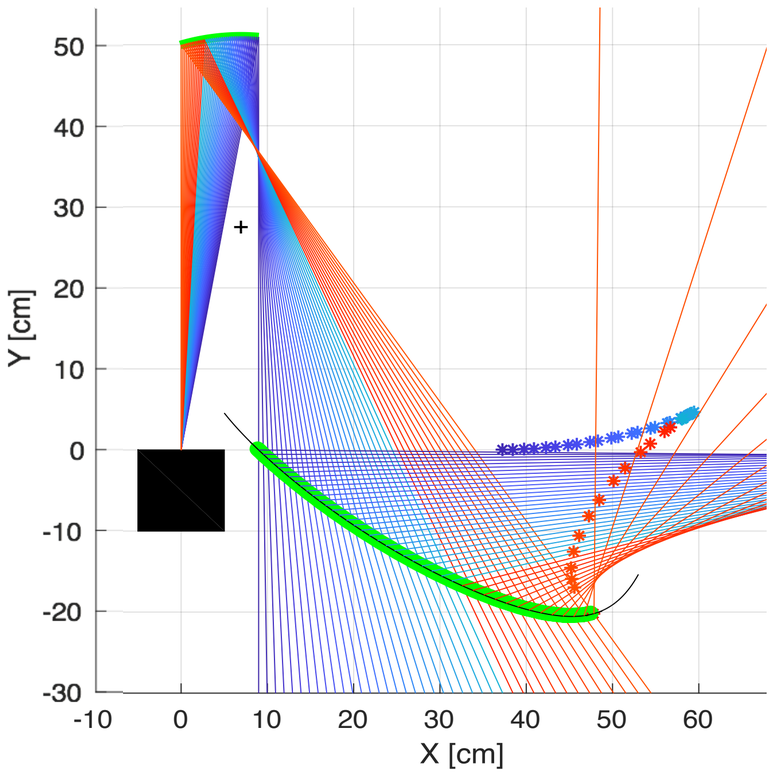

Fig.4. Design for *Secondary A*. The system is rotationally symmetric about the origin. Rays are traced by an ε step of .25°. For blue rays, ε = [3; 10]. For red rays, ε = [0; 3]. The red rays cover $\theta \pm 75°$. A polynomial of degree 10 is fit to the green piecewise quadratic surface. A focal point is plotted (asterisks) for each section of the primary mirror that intersects a given ray path.

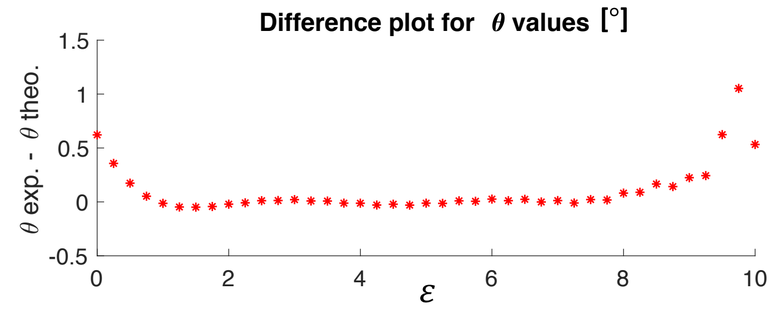

Fig.5. Error associated with experimental θ values for rays reflected from the derived polynomial for *Secondary* A, given theoretical values from Eq. 1. Mean difference $= .103°$.

Conclusions and Current Work

To further evaluate the design validity for a true all-sky distortionless image, we determine the depth of field that can be resolved for a given mirror system, detector and focusing lens. We take the field of view (FOV) for the camera to be 20°, using Eq. 3 to calculate the focal length of the lens. The FOV for the ideal design should include all focal points of the secondary mirror for at least rays $\theta = \pm 75°$. Focal points for the secondary mirror will be plotted using parallel ray tracing from the sky to the camera.

$$f = \frac{d}{2 * \tan(\varepsilon)}$$

Eq.3. For detector size $d = 12.8$ mm, and $\varepsilon = 10°$, $f = 36.3$ mm.

After many simulations for multiple secondary mirror surfaces, the most compact and well focused design will be manufactured.